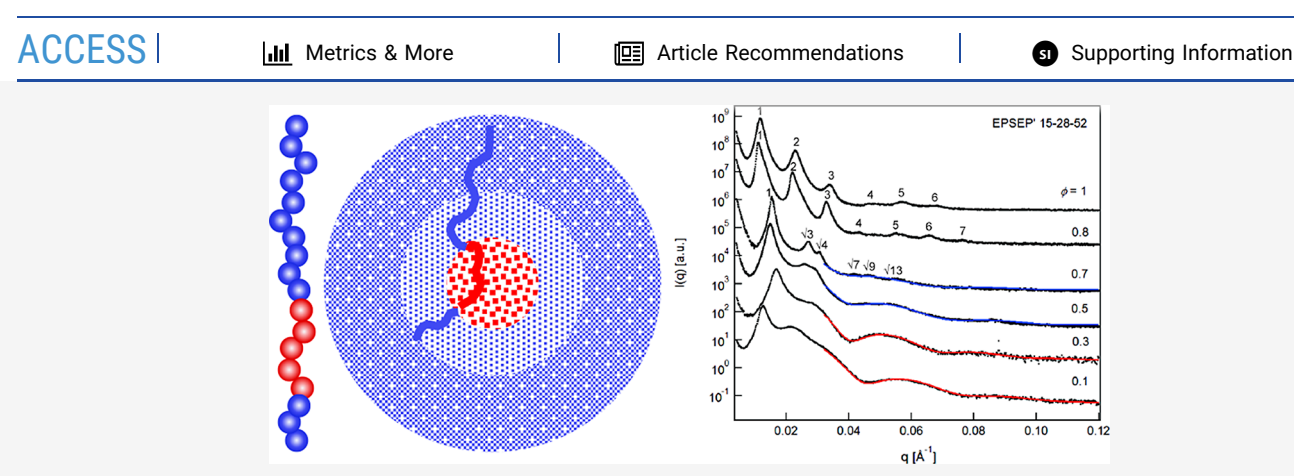


pubs.acs.org/Macromolecules Article

Solution and Bulk Structures of Asymmetric PEP-PS-PEP' Triblock Copolymers

Timothy P. Lodge,* En Wang, Jiahao Zhu, and Frank S. Bates*





ABSTRACT: The self-assembly of four polystyrene (S) and poly(ethylene-*alt*-propylene) (EP) block copolymers was studied in squalane, an EP-selective solvent. The polymers were prepared by sequential living anionic polymerization of isoprene and styrene, followed by catalytic hydrogenation of the diene block(s). The four polymers had comparable total molar masses (ca. 90 \pm 6 kg/mol) and volumetric compositions ($f_s \approx 0.25 \pm 0.01$) but different architectures. Specifically, a diblock SEP(26-70), a symmetric triblock EPSEP(30-24-30), and two asymmetric triblocks EPSEP'(8-26-62) and EPSEP'(15-28-52) were prepared, where the numbers denote block molar masses in kg/mol. Micellization in dilute solution (volume fraction $\phi \leq 0.01$) was studied by dynamic light scattering and small-angle X-ray scattering. All four polymers assembled into spherical micelles, and, as expected, the symmetric triblock formed the smallest particles. The results suggest that the asymmetric triblocks form micelles with a two-layer corona, the inner layer being enriched in the smaller endblock. Upon increasing concentration ($\phi = 0.1$ and 0.3), SEP(26-70) and EPSEP(30-24-30) micelles packed onto well-defined body-centered cubic lattices, also as expected. However, surprisingly, the asymmetric triblocks did not adopt a lattice at these volume fractions but rather retained a liquid-like packing. This remarkable effect of architecture was confirmed by linear viscoelastic measurements, which revealed striking differences between the asymmetric triblocks on one hand and the "conventional" architectures on the other. This behavior is speculated to arise from a different inter-micellar potential, stemming from the two-layer corona. At still higher concentrations, all four polymers adopted hexagonal packings, before transitioning to lamellae for $\phi \geq 0.8$.

■ INTRODUCTION

The self-assembly of block polymers in solution and bulk remains a topic of broad interest for many reasons, not the least of which is the ongoing discovery of unexpected new phenomena. A prime example is the recently revealed propensity for simple diblocks to select complex packings such as the Frank–Kasper and Laves phases. Other fruitful strategies for discovering new nanostructures include architectural variations, incorporation of three or more chemically distinct blocks, $^{10-14}$ and blending. On the other hand, in certain situations, it can be advantageous to suppress ordering, even at copolymer concentrations and molecular weights where the product of the total degree of polymerization, N, and the interaction parameter, χ , is well above the threshold for the order—disorder transition. By maintaining the sample in a disordered liquid-like state, mixing, formulation, or processing

can be facilitated. In this work, we exploit a simple architectural variation in ABA triblocks and disclose the surprising suppression of packing in concentrated solutions when the two endblocks A and A' have different lengths.

In the chosen system, the endblocks are poly(ethylene-alt-propylene) (EP), obtained by catalytic hydrogenation of 1,4-polyisoprene, and the midblock is polystyrene (S). Four polymers of nearly constant N and composition f_S are

Received: May 13, 2023 Revised: June 27, 2023 Published: August 2, 2023





Table 1. Polymer Characteristics

polymer	$M_{\rm n}$, PEP (kg/mol)	M _n , PS (kg/mol)	$M_{\rm n}$, PEP' (kg/mol)	Ð	$f_{ exttt{PS}}$	r
SEP(26-70)		26	70	1.04	0.24	0
EPSEP'(8-26-62)	8	26	62	1.05	0.24	0.13
EPSEP'(15-28-52)	15	28	52	1.04	0.26	0.29
EPSEP(30-24-30)	30	24	30	1.07	0.25	1

Table 2. Micelle Characteristics at 90 °C

polymer	$N_{ m agg}^{a}$	$R_{\rm core} \left({\rm nm} \right)^{b}$	$R_{\rm h}$ (nm)	μ_2/Γ^{2c}	$L_{ m corona}^{d}$ (nm)	CMT (°C)	$R_{\rm h}(190~^{\circ}{\rm C})/R_{\rm h}(90~^{\circ}{\rm C})^{e}$
SEP(26-70)	84 ± 5	9.2 ± 0.8	43 ± 2	0.08	34 ± 3	>200	0.9
EPSEP'(8-26-62)	75 ± 3	8.8 ± 0.9	42 ± 3	0.1	33 ± 2	>190	0.7
EPSEP'(15-28-52)	82 ± 9	9.6 ± 1.0	38 ± 4	0.1	28 ± 3	>190	0.5
EPSEP(30-24-30)	47 ± 5	7.5 ± 0.8	24 ± 1	0.06	17 ± 1	≈150	n/a

[&]quot;Computed from R_c assuming no solvent in the core. From SAXS fitting. Normalized second cumulant from DLS. Computed as $R_h - R_{core}$ Computed using data in Figure S3, confirming that the CMT decreases monotonically with r.

EXPERIMENTAL SECTION

Materials. All reagents were obtained from Sigma-Aldrich. One diblock, one symmetric triblock, and two asymmetric triblocks were prepared by sequential anionic polymerization of isoprene and styrene, followed by catalytic hydrogenation of the 1,4-polyisoprene (PI) block using a homogeneous Ni/Al catalyst under 400 psi H₂. The initiator was sec-butyllithium, the solvent was cyclohexane, and the polymerization temperature was 40 °C. Termination was achieved with degassed methanol. The hydrogenation was also carried out in cyclohexane at 77 °C; the catalyst was prepared by combining triethylaluminum and nickel 2-ethylhexanoate in the solvent, with a molar ratio of Al/Ni $\approx 2:1$. The polymer solution was typically 1-2 wt %, and the catalyst loading was about 1:10 with respect to moles of repeat units. In the case of the asymmetric triblocks, the shorter PI block was polymerized first. Further synthesis details can be found in previous publications.^{22–24} The polymers were characterized by a combination of ¹H NMR spectroscopy and size exclusion chromatography with multi-angle light scattering detection (SEC-MALS, Wyatt Technology DAWN). The first block molecular weight and dispersity were determined by SEC-MALS. The subsequent block molecular weights were determined via compositions from ¹H NMR spectroscopy, after narrow distributions were confirmed by SEC. The diblock was reported previously.²² The degree of saturation of the PI block was ≥99% in all cases. The resulting polymers are designated SEP(26-70), EPSEP(30-24-30), EPSEP'(8-26-62), and EPSEP'(15-28-52), where the numbers denote block molecular weights in kg/ mol. The total molecular weights and compositions are approximately constant, and the dispersities are reasonable, as indicated in Table 1. An asymmetry parameter, r, is defined as the ratio of the shorter to the longer EP block molecular weight, such that the diblock has r = 0 and the symmetric triblock has r = 1. Representative SEC traces are provided in Supporting Information, Figure S1.

Polymer solutions in squalane were prepared using dichloromethane as a cosolvent, which was allowed to evaporate at room temperature until constant weight was achieved. Dilute solutions for light scattering were filtered through 0.2 μ m PTFE filters to remove dust.

Dynamic Light Scattering. Dynamic light scattering (DLS) measurements were taken from room temperature to 190 °C, where room temperature measurements were obtained at angles from 60 to 120° in 15° increments, using a Brookhaven BI-200SM goniometer with wavelength $\lambda=637$ nm. Intensity autocorrelation functions were acquired for 20 min at each angle. High-temperature DLS measurements were performed on a home-built light scattering instrument, using a Brookhaven correlator and $\lambda=488$ nm. Data were acquired at an angle of 90°. Correlation functions were analyzed by the method of cumulants, 25 to obtain the mean decay rate and its dispersity, and by the regularized positive exponential sum (REPES) inverse Laplace transform method. Typically, $\phi \leq 0.005$ (≈ 5 mg/mL) or even lower concentrations were prepared to avoid micelle overlap. Mean decay rates were converted to hydrodynamic radii $R_{\rm h}$ by the Stokes–Einstein–Sutherland relation.

Small-Angle X-ray Scattering. Small-angle X-ray scattering (SAXS) was performed at the 5-ID-D beam line at the DuPont-Northwestern-Dow (DND-CAT) station at the Argonne National Laboratory. A beam energy of 17 keV, corresponding to $\lambda = 0.73$ Å, and a sample-to-detector distance of 8.5 m were selected to give a wavevector range of $0.003 \le q \le 0.15 \text{ Å}^{-1}$, where $q = 4\pi\lambda^{-1}\sin(\theta/2)$, with θ being the scattering angle. Due to the high flux, only 1 s exposure times were required, even for dilute micelle solutions. Solution samples ($\phi \leq 0.1$) were loaded and sealed into capillary tubes after the co-solvent procedure. Concentrated micelle solutions $(\phi > 0.1)$ were loaded into hermetic aluminum pans by solvent casting and then sealed under argon in a glovebox. A 16-position capillary stage was available for room temperature, while an 8-position hot capillary stage was used for temperatures from 25 to 200 °C. A 32-position stage was employed for heating and cooling samples in aluminum pans. At each temperature, samples were annealed for 10 min to equilibrate thermally and then exposed to X-rays. A pure solvent sample was measured as a background to be subtracted from micelle solution scattering. Since the samples are isotropic, twodimensional scattering images were azimuthally averaged to the onedimensional intensity I(q) vs q in arbitrary intensity units.

Rheology. Rheological experiments were performed on a rotational rheometer (ARES, TA Instruments) with 25 mm diameter parallel plates. Concentrated (ϕ > 0.1) micelle solutions were loaded at 120 °C under nitrogen, filling the gap (\approx 1 mm) between two parallel plates. Samples were first tested on a strain–sweep mode (0.1–100%) to find the extent of the linear regime. At an appropriate strain amplitude (typically 1–10%), samples underwent frequency sweeps from 100 to 0.1 rad/s at multiple temperatures from 30 to 150

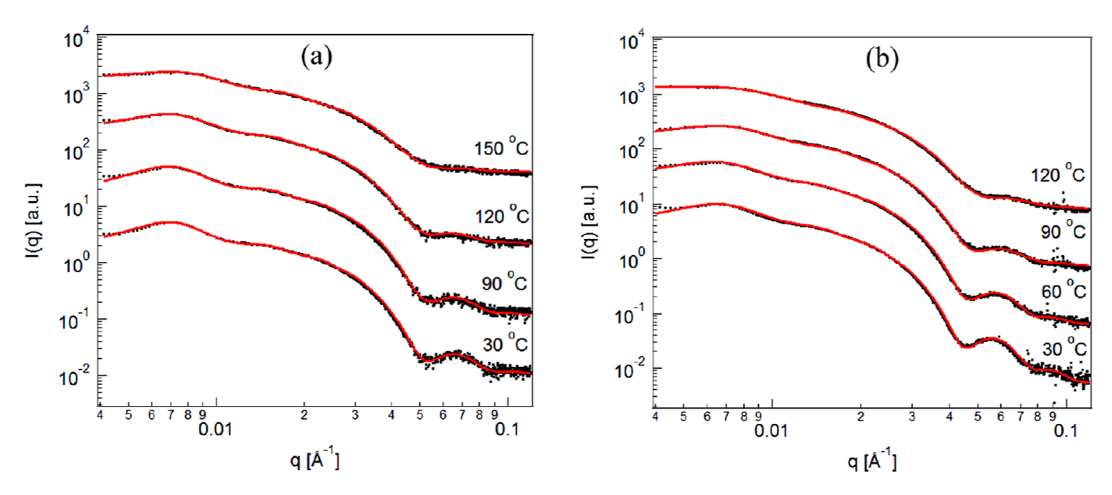


Figure 1. SAXS patterns and model fits for $\phi = 0.01$ solutions of (a) EPSEP'(8-26-62) and (b) EPSEP'(15-28-52) triblock micelles at multiple temperatures. Note that data at different temperatures are vertically shifted for clarity.

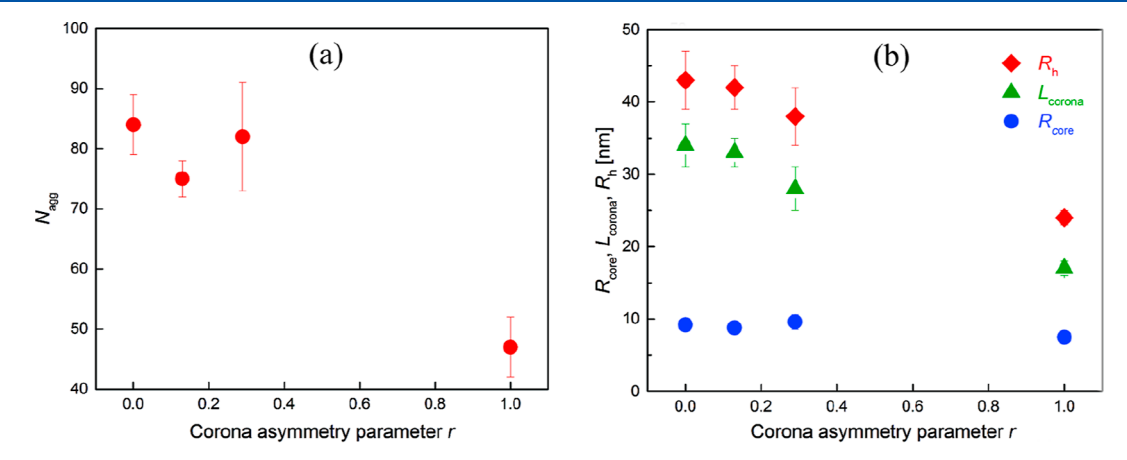


Figure 2. Micelle characteristics at 90 °C: (a) aggregation numbers and (b) core radius, corona thickness, and hydrodynamic radius, as a function of the asymmetry parameter.

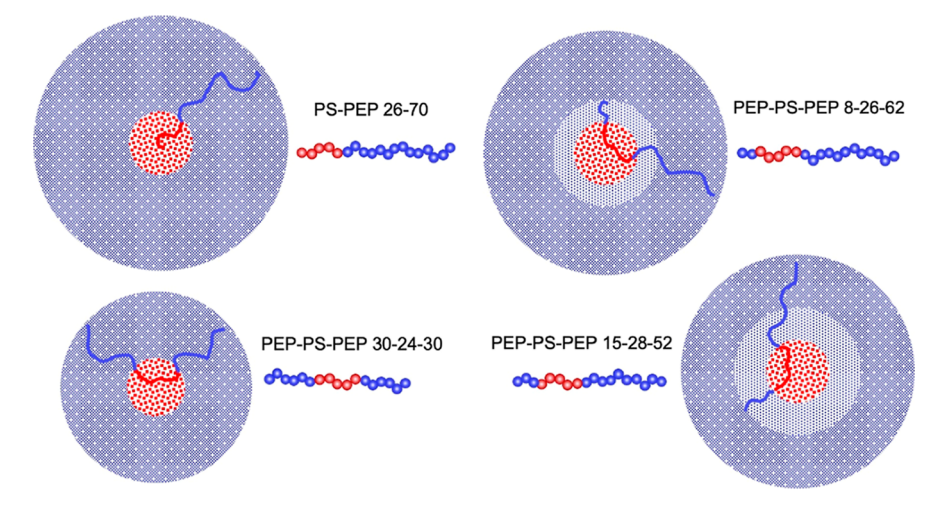


Figure 3. Cartoon of chain packing into spherical micelles, emphasizing the assumed formation of an inner corona layer containing the shorter PEP blocks.

RESULTS

Dilute Solutions. All four copolymers formed spherical micelles with narrow size distributions (dispersity ≤ 1.1) in

dilute solution. DLS provided the mean hydrodynamic radius, $R_{\rm h}$, and associated dispersity. REPES analysis confirmed monomodal and narrow size distributions (see Supporting Information, Figure S2). Temperature-dependent DLS was used to obtain the approximate location of the critical micelle

 $^{^{\}circ}$ C. At each temperature, samples were annealed for 10 min to thermally equilibrate before dynamic shear measurements.

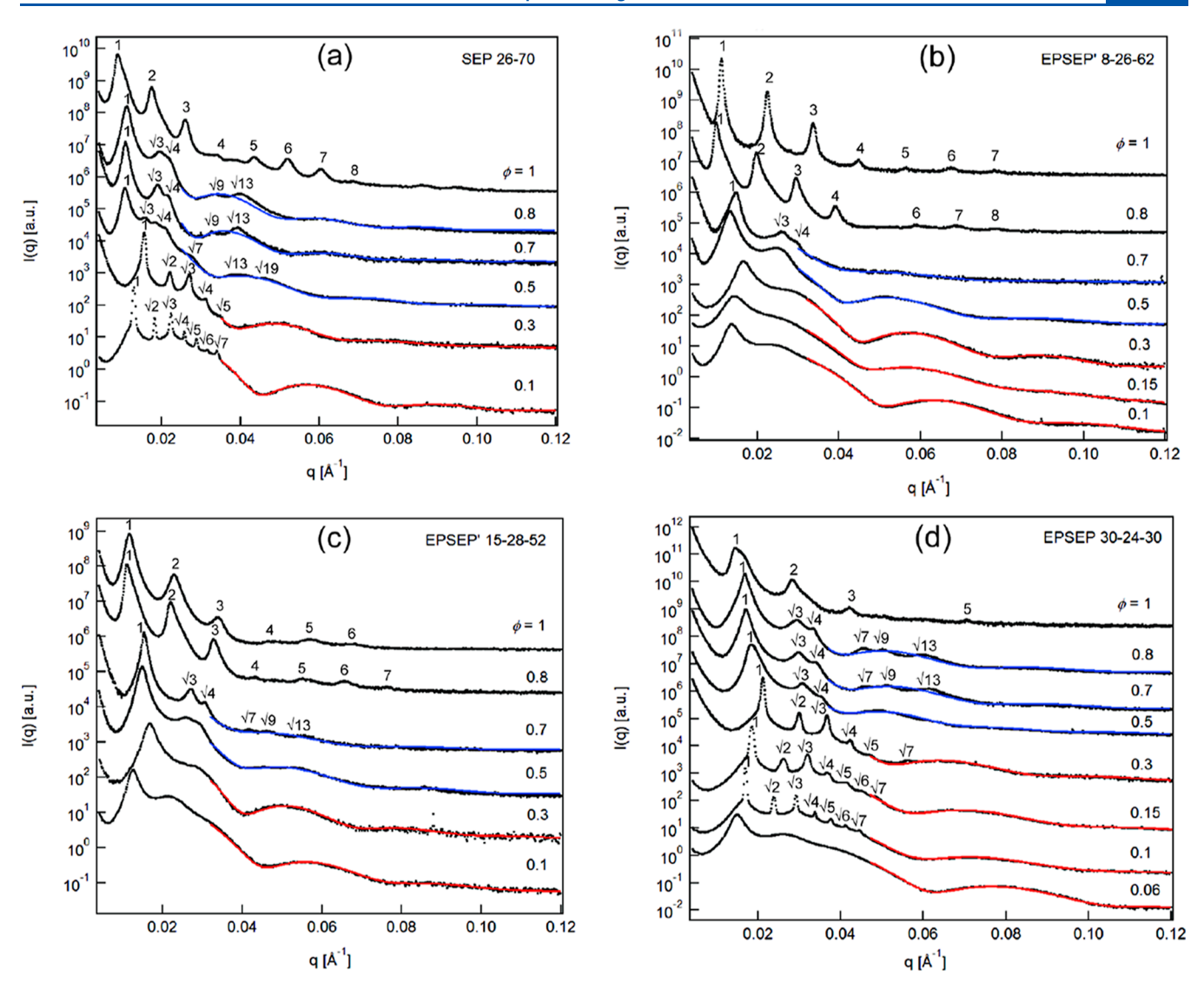


Figure 4. SAXS patterns and fits to particle form factors of (a) SEP(26-70) diblock and (b) EPSEP'(8-26-62), (c) EPSEP'(15-28-52), and (d) EPSEP(30-24-30) triblock copolymer solutions at different polymer volume fractions φ. Measurements were taken at 120 °C. Red and blue curves indicate fits to spherical and cylindrical form factors, respectively.

temperature (CMT), as shown in Supporting Information, Figure S3. The micelle characteristics are collected in Table 2.

SAXS profiles for dilute solutions of the two asymmetric triblocks at four selected temperatures are shown in Figure 1; qualitatively similar curves for the diblock and symmetric triblock have been obtained previously. The first minimum associated with a spherical core form factor is clearly evident, although the core—corona interface becomes progressively less sharp as the temperature increases. A weak maximum associated with a hard sphere structure factor is also visible at lower q. All of the curves are well-described by a micelle form factor model with the Percus—Yevick structure factor (see the Supporting Information for details). The key parameter is the radius of the core, $R_{\rm core}$, which is used to compute the micelle aggregation number, $N_{\rm agg}$ under the assumption of a "dry" core. The corona thickness, $L_{\rm corona}$, can also be estimated as $R_{\rm h}-R_{\rm core}$.

These various size parameters are plotted as functions of the asymmetry parameter, r, in Figure 2. The symmetric triblock (r = 1) forms the smallest micelles and the diblock (r = 0) forms the largest. This result confirms a previous work, ²³ and it is

well-understood that each triblock has two corona chains, thereby increasing the corona crowding and favoring a lower N_{agg} , compared to that of a diblock with the same N_{core} . Consistent with this, the symmetric triblock has the lowest CMT, ca. 150 °C, and the diblock has the highest (>200 °C). The two asymmetric triblocks fall in between in terms of size and CMT, but both are much closer to the diblock. This result suggests two possibilities: the smaller PEP block inserts into the core, or the smaller PEP block forms an inner corona layer, allowing the larger PEP block to find much more conformational freedom in a relatively dilute outer corona. This latter situation is depicted in cartoon form in Figure 3. An intermediate state between these limits is also conceivable. However, based on the molecular weights of the shorter PEP blocks, 8 and 15 kDa, it seems very unlikely that there is significant insertion into the core. Partial insertion also seems unlikely, based on the well-defined spherical form factor minima at lower temperatures; partial insertion would lead to a broad interface, smearing the form factor minimum. Finally, the packing of the micelles at higher concentrations, to be

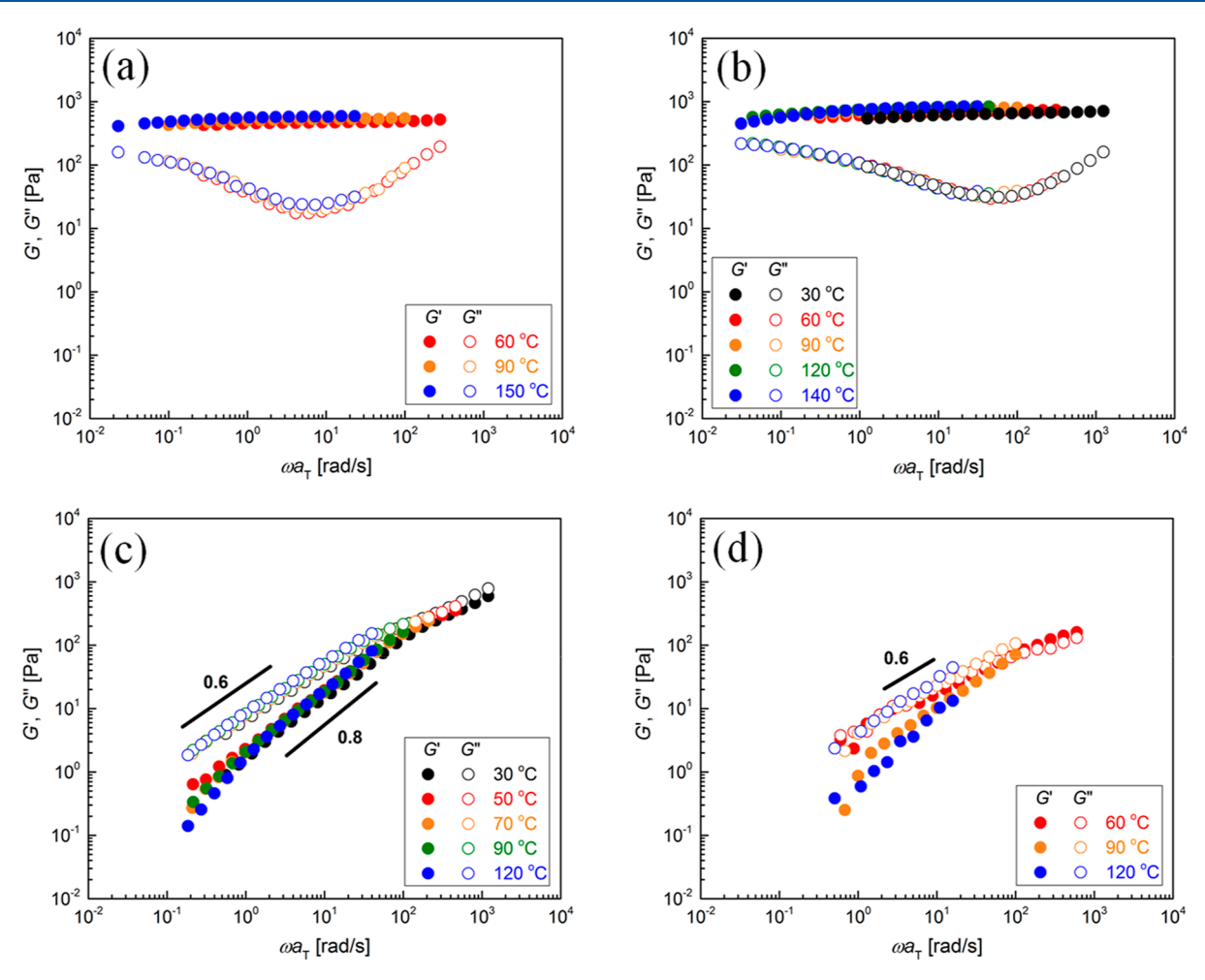


Figure 5. Storage and loss modulus vs frequency master curves at a polymer volume fraction $\phi = 0.1$ for (a) SEP(26-70), (b) EPSEP(30-24-30), (c) EPSEP'(8-26-62), and (d) EPSEP'(15-28-52).

presented next, also argues against full insertion as the behavior is quite different from that of the diblock.

Concentrated Solutions. The packing of chains was examined by SAXS for higher volume fractions, ranging from ϕ = 0.1 to the melt (ϕ = 1). Representative traces are shown for all four polymers at 120 °C in Figure 4. The diblock (Figure 4a) and symmetric triblock (Figure 4d) behave as expected; namely, they exhibit a well-defined BCC lattice at $\phi = 0.1$ and ϕ = 0.3, hexagonal packing (HEX) at ϕ = 0.5, 0.7, and 0.8, and lamellae (LAM) in the melt. 20,21,30,31 Measurements were not taken at enough concentrations to assess whether the double gyroid phase appears between HEX and LAM. In contrast, the two asymmetric triblocks are quite different (Figure 4b,c). No BCC peaks are evident at ϕ = 0.1 and ϕ = 0.3. Instead, the profiles retain the signature of spherical cores (red fitted curves) with an increasingly prominent structure factor peak, indicative of a liquid-like packing of spheres. At $\phi = 0.5$ and ϕ = 0.7, there is evidence of hexagonal packing of cylinders, including form factor oscillations (blue fitted curves), similar to those of the diblock and symmetric triblock. However, the asymmetric triblocks form well-defined lamellae at $\phi = 0.8$, whereas the other two polymers are still in a hexagonal phase. Note that all the samples were annealed for extended periods well above the glass transition of the core blocks. Failure to pack onto a lattice is most apparent at the lower polymer concentrations. Both of these features argue strongly that the unusual behavior of the asymmetric triblocks is not a simple kinetic effect. Also, in measurements³² and simulations³³ documented elsewhere, time-resolved chain exchange measurements on these polymers in dilute solution indicate that the asymmetric triblocks exchange between micelles more rapidly than the diblocks, again indicating that chain mobility alone is not an important contribution to the observed failure to pack on a lattice. Furthermore, all four polymers have similar total molecular weights and compositions, so the difference in packing must be attributed entirely to the asymmetric architecture.

Viscoelastic properties also provide compelling evidence of a profound difference in packing between the asymmetric triblocks on one hand, and the diblock and symmetric triblock on the other. Figures 5 and 6 show time—temperature superposed master curves for all four polymers, at $\phi=0.1$ and $\phi=0.3$, respectively. The superposition is not perfect, as expected, but still quite reasonable, indicating that there are no substantial changes in the structure with temperature in any of these samples. The diblock and symmetric triblock show clear plateaus in the elastic modulus G' (Figures 5a,b and 6a,b), consistent with cubic packing, as discussed in detail elsewhere. The symmetric polymers show no hint of a plateau but rather approximately power law behavior with non-canonical exponents. Importantly, the magnitudes of the lower frequency moduli are much smaller for the asymmetric

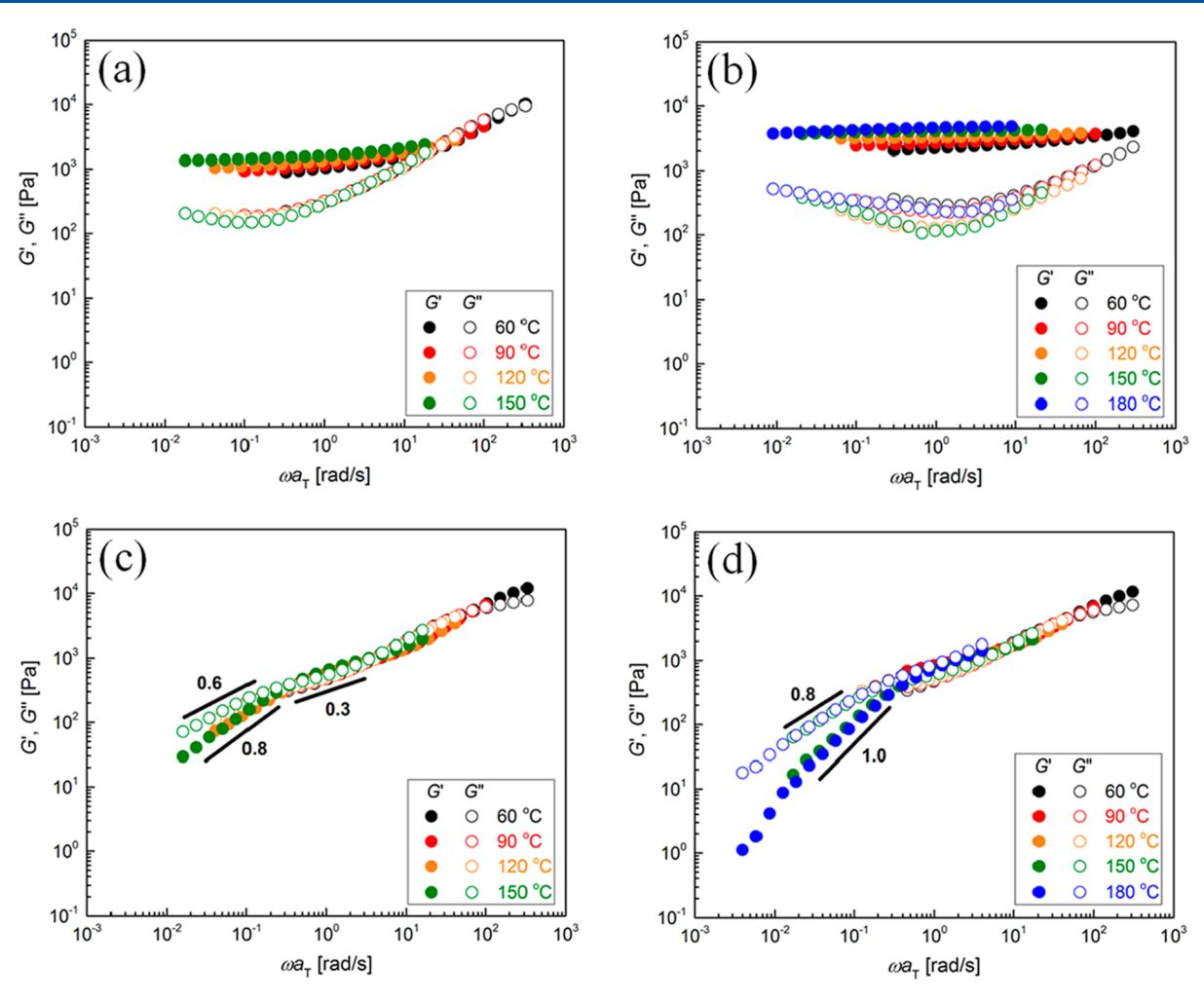


Figure 6. Storage and loss modulus vs frequency master curves at a polymer volume fraction $\phi = 0.3$ for (a) SEP(26-70), (b) EPSEP(30-24-30), (c) EPSEP'(8-26-62), and (d) EPSEP'(15-28-52).

systems, typically by 1 to 2 orders of magnitude, suggestive of a more liquid-like state and consistent with the SAXS results.

DISCUSSION

Having established a remarkable phenomenon that asymmetric triblock copolymer micelles do not pack on a BCC lattice, whereas diblocks and symmetric triblocks of comparable concentration, composition, and total molar mass do, it is appropriate to consider possible explanations. For the reasons noted previously, we can discount simple kinetic limitations as a significant contributor. The next possibility is that the micelles formed by the asymmetric triblocks are too disperse in size to adopt a BCC packing, in which each lattice site is necessarily equivalent. From DLS analysis (Table 1), the dispersity of the asymmetric polymer micelles is about 1.1, compared to 1.08 for the diblocks and 1.06 for the symmetric triblocks. However, the SAXS profiles indicate qualitatively similar form factor minima among the four polymers, suggesting that micelle core dispersity does not vary significantly among the samples. Furthermore, the relatively rapid chain exchange of the asymmetric triblocks should be able to mitigate any deleterious effects of micelle size dispersity; the molecular dispersity is small and comparable across the four samples. The extensive literature on block copolymers in concentrated solutions and melts indicates that molecular dispersity does not inhibit packing onto a lattice,

although it can certainly modulate the choice of lattice and its dimensions.^{35–38} Therefore, we are inclined to discount this possibility. However, it should be possible in the future to make self-consistent mean field (SCFT) calculations to explore whether modest dispersity exhibits an unexpectedly large effect for asymmetric triblocks.

A further possibility is that the micelles formed by the asymmetric triblocks are actually ellipsoidal in shape. For example, consider a prolate ellipsoid. If the longer PEP blocks were to locate preferentially at the poles, where the curvature is higher, the corona crowding penalty would be reduced, while the shorter corona blocks could be distributed more toward the micelle equator. The same argument could be applied to an oblate ellipsoid, with the larger PEP blocks preferentially located around the rim. However, in either case, this benefit would be countered by an increase in interfacial area plus a modest decrease in mixing entropy of the endblocks. Clearly, from the success of the spherical form factor fits to the SAXS data, the eccentricity of any ellipsoidal particle would have to be rather subtle. This is a difficult hypothesis to test experimentally; DLS, for example, gives no direct information about shape. It is possible that simulations could provide insights as to how much eccentricity of soft particles would be required to suppress packing onto a BCC lattice. On the whole, however, we do not believe that this is the correct explanation.

The third possibility, and the one that appears the most plausible, is that the concentration of PEP monomers as a function of distance away from the core-corona interface varies in a way that is significantly different for the "bimodal brush". This possibility is suggested by the cartoons in Figure 3; the location of the shorter PEP blocks in an inner corona layer could lead to an inter-micellar potential with a very soft outer region and a denser interior zone. Conceivably, such a profile does not favor BCC but some other micellar packing.^{39,40} Candidates could include one of the Frank-Kasper or Laves phases, recently extensively documented in diblock copolymer sphere packings, such as σ , A15, C14, and C15, which are characterized by unit cells containing micelles of 5, 2, 3, and 2 different sizes, respectively. In the future, SCFT could be used to explore whether these architectural variations lead to a change in relative free energies of various sphere packings. However, it is important to bear in mind that SCFT cannot address the free energy of the liquid-like packing observed, and thus, we cannot directly address whether these samples are trapped in a metastable state. Even if chain exchange were relatively facile, the time to adopt such a complicated packing could be substantial.⁴¹ In contrast, closepacked phases such as face-centered cubic and hexagonally close-packed, which have been amply documented in spherical block copolymer micelles, 42-46 feature a single micelle size and no extra kinetic barriers to their formation.

SUMMARY

The self-assembly of two asymmetric ABA' triblocks has been examined, from dilute solution in a selective solvent up to the melt. The results are compared in detail to a diblock and a symmetric triblock, all four polymers having very comparable total molar mass and compositions. All four polymers form spherical micelles in dilute solution ($\phi \leq 0.01$), with the hydrodynamic radius decreasing with increasing asymmetry parameter r (defined as the ratio of the shorter to the longer endblock). This result is consistent with the asymmetric triblocks forming a "two-layer" corona, with the shorter endblock enriched in the inner layer. At the other extreme, in the melt, all four polymers form lamellae. At intermediate concentrations, however, the results are quite distinct. Whereas the diblock (r = 0) and the symmetric triblock (r = 1) readily form well-defined BCC packings at $\phi = 0.1$ and 0.3, the asymmetric triblocks retain a liquid-like packing until $\phi \approx 0.5$. These SAXS results are corroborated by linear viscoelastic measurements, which confirm the solid-like nature of the BCC samples versus more liquid-like dynamic moduli for the asymmetric systems. Possible explanations for these observations are considered; the most likely appears to be that the modified inter-micellar potential for the asymmetric triblocks destabilizes the BCC packing. Potentially, the system would prefer a more elaborate structure, such as a Frank-Kasper or Laves phase, in which the necessity of forming distinct micelle populations with different aggregation numbers could provide a substantial kinetic barrier to ordering. In any event, this system demonstrates a rather straightforward strategy for retaining liquid-like structures at copolymer molar masses and concentrations where ordering would be expected, which could be advantageous for processing and formulation.

ASSOCIATED CONTENT

Supporting Information

The Supporting Information is available free of charge at https://pubs.acs.org/doi/10.1021/acs.macromol.3c00931.

SEC traces of triblock copolymers; REPES analysis of micelles; estimation of CMT for micelles; and details of SAXS fitting to the micelle structure and form factors (PDF)

AUTHOR INFORMATION

Corresponding Authors

Timothy P. Lodge — Department of Chemistry and Department of Chemical Engineering & Materials Science, University of Minnesota, Minneapolis, Minnesota 55455, United States; ⊚ orcid.org/0000-0001-5916-8834; Email: lodge@umn.edu

Frank S. Bates — Department of Chemical Engineering & Materials Science, University of Minnesota, Minneapolis, Minnesota 55455, United States; oorcid.org/0000-0003-3977-1278; Email: bates001@umn.edu

Authors

En Wang — Department of Chemical Engineering & Materials Science, University of Minnesota, Minneapolis, Minnesota 55455, United States; orcid.org/0000-0002-3271-7562

Jiahao Zhu — Department of Chemical Engineering & Materials Science, University of Minnesota, Minneapolis, Minnesota 55455, United States; orcid.org/0000-0003-1534-4618

Complete contact information is available at: https://pubs.acs.org/10.1021/acs.macromol.3c00931

Notes

The authors declare no competing financial interest.

ACKNOWLEDGMENTS

This work was supported in part by Infineum, L.L.P. SAXS experiments were performed at the 5-ID-D beamline of the Dupont—Northwestern—Dow Access Team (DND-CAT) at the Advanced Photon Source (APS), Argonne National Laboratory. Use of the APS, an Office of Science User Facility operated for the U.S. Department of Energy (DOE) Office of Science by the Argonne National Laboratory, was supported by the U.S. DOE under contract no. DE-AC02-06CH11357. The authors acknowledge the Characterization Facility, College of Science and Engineering, University of Minnesota, which receives partial support from the NSF through the MRSEC (Award Number DMR-2011401) and the NNCI (Award Number ECCS-2025124) programs.

REFERENCES

- (1) Bates, C. M.; Bates, F. S. 50th Anniversary Perspective: Block Polymers—Pure Potential. Macromolecules 2017, 50, 3-22.
- (2) Lee, S.; Bluemle, M. J.; Bates, F. S. Discovery of a Frank-Kasper σ Phase in Sphere-Forming Block Copolymer Melts. *Science* **2010**, 330, 349–353.
- (3) Xie, N.; Li, W.; Qiu, F.; Shi, A.-C. σ Phase Formed in Conformationally Asymmetric AB-Type Block Copolymers. *ACS Macro Lett.* **2014**, *3*, 906–910.
- (4) Kim, K.; Arora, A.; Lewis, R. M., 3rd; Liu, M.; Li, W.; Shi, A. C.; Dorfman, K. D.; Bates, F. S. Origins of Low-Symmetry Phases in Asymmetric Diblock Copolymer Melts. *Proc. Natl. Acad. Sci. U.S.A.* **2018**, *115*, 847–854.

- (5) Bates, M. W.; Lequieu, J.; Barbon, S. M.; Lewis, R. M., III; Delaney, K. T.; Anastasaki, A.; Hawker, C. J.; Fredrickson, G. H.; Bates, C. M. Stability of the A15 Phase in Diblock Copolymer Melts. *Proc. Natl. Acad. Sci. U.S.A.* **2019**, *116*, 13194–13199.
- (6) Milner, S. T. Chain Architecture and Asymmetry in Copolymer Microphases. *Macromolecules* **1994**, *27*, 2333–2335.
- (7) Tselikas, Y.; Iatrou, H.; Hadjichristidis, N.; Liang, K. S.; Mohanty, K.; Lohse, D. J. Morphology of miktoarm star block copolymers of styrene and isoprene. *J. Chem. Phys.* **1996**, *105*, 2456–2462.
- (8) Minehara, H.; Pitet, L. M.; Kim, S.; Zha, R. H.; Meijer, E. W.; Hawker, C. J. Branched Block Copolymers for Tuning of Morphology and Feature Size in Thin Film Nanolithography. *Macromolecules* **2016**, 49, 2318–2326.
- (9) Huang, K.; Rzayev, J. Well-Defined Organic Nanotubes from Multicomponent Bottlebrush Copolymers. *J. Am. Chem. Soc.* **2009**, 131, 6880–6885.
- (10) Mogi, Y.; Nomura, M.; Kotsuji, H.; Ohnishi, K.; Matsushita, Y.; Noda, I. Superlattice Structures in Morphologies of the ABC Triblock Copolymers. *Macromolecules* **1994**, *27*, 6755–6760.
- (11) Stadler, R.; Auschra, C.; Beckmann, J.; Krappe, U.; Voight-Martin, I.; Leibler, L. Morphology and Thermodynamics of Symmetric Poly(A-block-B-block-C) Triblock Copolymers. *Macromolecules* 1995, 28, 3080–3097.
- (12) Bailey, T. S.; Hardy, C. M.; Epps, T. H.; Bates, F. S. A Noncubic Triply Periodic Network Morphology in Poly(isoprene-b-styrene-b-ethylene oxide) Triblock Copolymers. *Macromolecules* **2002**, *35*, 7007–7017.
- (13) Chanpuriya, S.; Kim, K.; Zhang, J.; Lee, S.; Arora, A.; Dorfman, K. D.; Delaney, K. T.; Fredrickson, G. H.; Bates, F. S. Cornucopia of Nanoscale Ordered Phases in Sphere-Forming Tetrablock Terpolymers. ACS Nano 2016, 10, 4961–4972.
- (14) Bates, F. S.; Hillmyer, M. A.; Lodge, T. P.; Bates, C. M.; Delaney, K. T.; Fredrickson, G. H. Multiblock Polymers: Panacea or Pandora's Box? *Science* **2012**, *336*, 434–440.
- (15) Mueller, A. J.; Lindsay, A. P.; Jayaraman, A.; Weigand, S.; Lodge, T. P.; Mahanthappa, M. K.; Bates, F. S. Tuning Diblock Copolymer Particle Packing with Variable Molecular Weight Core-Homopolymer. *Macromolecules* **2022**, *55*, 8332–8344.
- (16) Lindsay, A. P.; Cheong, G. K.; Peterson, A. J.; Weigand, S. J.; Dorfman, K. D.; Lodge, T. P.; Bates, F. S. Complex Phase Behavior in Particle-Forming AB/AB' Diblock Copolymer Blends with Variable Core Block Lengths. *Macromolecules* **2021**, *54*, 7088–7101.
- (17) Xie, S.; Lindsay, A. P.; Bates, F. S.; Lodge, T. P. Formation of a C15 Laves Phase with a Giant Unit Cell in Salt-Doped A/B/AB Ternary Polymer Blends. ACS Nano 2020, 14, 13754–13764.
- (18) Quintana, J. R.; Villacampa, M.; Muñoz, M.; Andrio, A.; Katime, I. A. Micellization of a polystyrene-block-poly(ethylene/propylene) copolymer in n-alkanes. 1. Thermodynamic study. *Macromolecules* **1992**, *25*, 3125–3128.
- (19) Quintana, J. R.; Villacampa, M.; Andrio, A.; Muñoz, M.; Katime, I. A. Micellization of a polystyrene-block-poly(ethylene/propylene) copolymer in n-alkanes. 2. Structural study. *Macromolecules* 1992, 25, 3129–3136.
- (20) Lai, C.; Russel, W. B.; Register, R. A. Phase Behavior of Styrene—Isoprene Diblock Copolymers in Strongly Selective Solvents. *Macromolecules* **2002**, *35*, 841–849.
- (21) Choi, S.; Bates, F. S.; Lodge, T. P. Structure of Poly(styrene-bethylene-alt-propylene) Diblock Copolymer Micelles in Squalane. *J. Phys. Chem. B* **2009**, *113*, 13840–13848.
- (22) Choi, S.; Lodge, T. P.; Bates, F. S. Mechanism of Molecular Exchange in Diblock Copolymer Micelles: Hypersensitivity to Core Chain Length. *Phys. Rev. Lett.* **2010**, *104*, 047802–047804.
- (23) Lu, J.; Bates, F. S.; Lodge, T. P. Remarkable Effect of Molecular Architecture on Chain Exchange in Triblock Copolymer Micelles. *Macromolecules* **2015**, 48, 2667–2676.
- (24) Wang, E.; Lu, J.; Bates, F. S.; Lodge, T. P. Effect of Corona Block Length on the Structure and Chain Exchange Kinetics of Block Copolymer Micelles. *Macromolecules* **2018**, *51*, 3563–3571.

- (25) Koppel, D. E. Analysis of Macromolecular Polydispersity in Intensity Correlation Spectroscopy: The Method of Cumulants. *J. Chem. Phys.* **1972**, *57*, 4814–4820.
- (26) Jakes, J. Regularized Positive Exponential Sum (REPES) Program A Way of Inverting Laplace Transform Data Obtained by Dynamic Light Scattering. *Collect. Czech. Chem. Commun.* **1995**, *60*, 1781–1797.
- (27) Pedersen, J. S.; Gerstenberg, M. C. Scattering Form Factor of Block Copolymer Micelles. *Macromolecules* **1996**, 29, 1363–1365.
- (28) Pedersen, J. S.; Svaneborg, C. Scattering from Block Copolymer Micelles. *Curr. Opin. Colloid Interface Sci.* **2002**, *7*, 158–166.
- (29) Bang, J.; Viswanathan, K.; Lodge, T. P.; Park, M. J.; Char, K. Temperature-Dependent Micellar Structures in Poly(styrene-b-isoprene) Diblock Copolymer Solutions near the Critical Micelle Temperature. *J. Chem. Phys.* **2004**, *121*, 11489–11500.
- (30) Hanley, K. J.; Lodge, T. P.; Huang, C. I. Phase Behavior of a Block Copolymer in Solvents of Varying Selectivity. *Macromolecules* **2000**, 33, 5918–5931.
- (31) Lodge, T. P.; Pudil, B.; Hanley, K. J. The Full Phase Behavior for Block Copolymers in Solvents of Varying Selectivity. *Macromolecules* **2002**, *35*, 4707–4717.
- (32) Wang, E. Ph.D. Thesis, University of Minnesota-Twin Cities, 2019.
- (33) Peters, A. J.; Lodge, T. P. Chain Exchange Kinetics of Asymmetric B₁AB₂ Linear Triblock and AB₁B₂ Branched Triblock Copolymers. *Macromolecules* **2017**, *50*, 6303–6313.
- (34) Kossuth, M. B.; Morse, D. C.; Bates, F. S. Viscoelastic behavior of cubic phases in block copolymer melts. *J. Rheol.* **1999**, 43, 167–196
- (35) Lynd, N. A.; Hillmyer, M. A. Influence of Polydispersity on the Self-Assembly of Diblock Copolymers. *Macromolecules* **2005**, *38*, 8803–8810.
- (36) Meuler, A. J.; Ellison, C. J.; Qin, J.; Evans, C. M.; Hillmyer, M. A.; Bates, F. S. Polydispersity effects in poly(isoprene-b-styrene-bethylene oxide) triblock terpolymers. *J. Chem. Phys.* **2009**, *130*, 234903.
- (37) Widin, J. M.; Schmitt, A. K.; Schmitt, A. L.; Im, K.; Mahanthappa, M. K. Unexpected Consequences of Block Polydispersity on the Self-Assembly of ABA Triblock Copolymers. *J. Am. Chem. Soc.* **2012**, *134*, 3834–3844.
- (38) Hustad, P. D.; Marchand, G. R.; Garcia-Meitin, E. I.; Roberts, P. L.; Weinhold, J. D. Photonic Polyethylene from Self-Assembled Mesophases of Polydisperse Olefin Block Copolymers. *Macromolecules* **2009**, *42*, 3788–3794.
- (39) Likos, C. N. Effective interactions in soft condensed matter physics. *Phys. Rep.* **2001**, 348, 267–439.
- (40) Grason, G. M. The packing of soft materials: Molecular asymmetry, geometric frustration and optimal lattices in block copolymer melts. *Phys. Rep.* **2006**, 433, 1–64.
- (41) Lindsay, A. P.; Jayaraman, A.; Peterson, A. J.; Mueller, A. J.; Weigand, S. J.; Almdal, K.; Mahanthappa, M.; Lodge, T. P.; Bates, F. S. Reevaluation of Poly(ethylene-alt-propylene)-block-Polydimethylsiloxane Phase Behavior Uncovers Topological Close-Packing and Epitaxial Quasicrystal Growth. ACS Nano 2021, 15, 9453—9468.
- (42) Bang, J.; Lodge, T. P.; Wang, X.; Brinker, K. L.; Burghardt, W. R. Thermoreversible, Epitaxial, Close-Packed↔BCC Transitions in Block Copolymer Solutions. *Phys. Rev. Lett.* **2002**, *89*, 215505.
- (43) Bang, J.; Lodge, T. P. Mechanisms and Epitaxial Relationships between Close-Packed and BCC Lattices in Block Copolymer Solutions. *J. Phys. Chem. B* **2003**, *107*, 12071–12081.
- (44) McConnell, G. A.; Gast, A. P. Melting of Ordered Arrays and Shape Transitions in Highly Concentrated Diblock Copolymer Solutions. *Macromolecules* **1997**, *30*, 435–444.
- (45) Huang, Y. Y.; Hsu, J. Y.; Chen, H. L.; Hashimoto, T. Existence of fcc-Packed Spherical Micelles in Diblock Copolymer Melt. *Macromolecules* **2007**, *40*, 406–409.
- (46) Park, M.-J.; Bang, J.; Harada, T.; Char, K.; Lodge, T. P. Epitaxial Transitions Among FCC, HCP, BCC, and Cylinder Phases in a Block Copolymer Solution. *Macromolecules* **2004**, *37*, 9064–9075.